Suppl Fig. 1

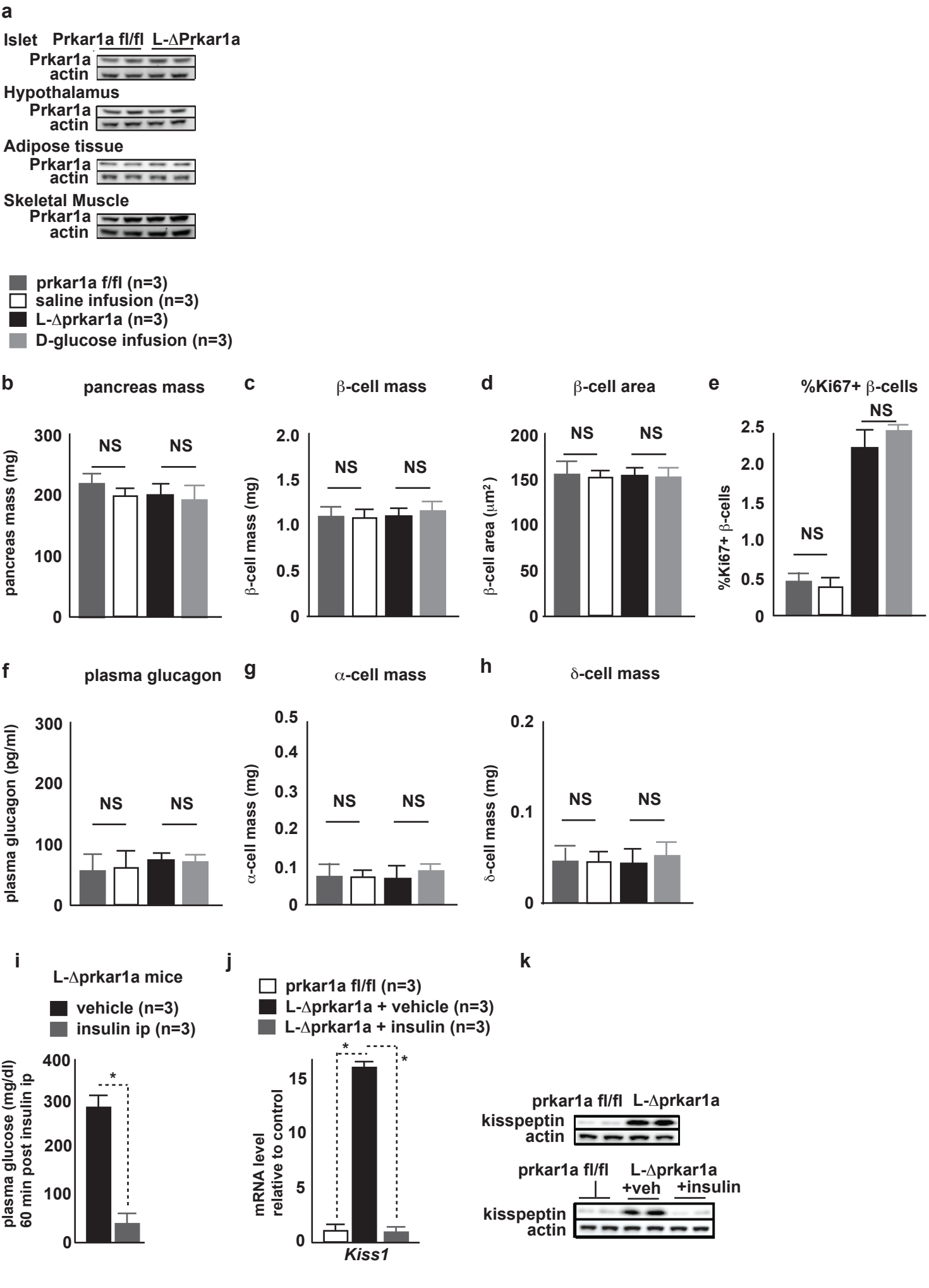
a
Islet
Prkar1a fl/fl
L-ΔPrkar1a
Prkar1a
actin
Hypothalamus
Prkar1a
actin
Adipose tissue
Prkar1a
actin
Skeletal Muscle
Prkar1a
actin
prkar1a f/fl (n=3)
saline infusion (n=3)
L-Δprkar1a (n=3)
D-glucose infusion (n=3)
b
pancreas mass
pancreas mass (mg)
300
200
100
0
NS
NS
c
β-cell mass
β-cell mass (mg)
2.0
1.5
1.0
0.5
0
NS
NS
d
β-cell area
β-cell area (μm²)
200
150
100
50
0
NS
NS
e
%Ki67+ β-cells
%Ki67+ β-cells
2.5
2.0
1.5
1.0
0.5
0
NS
NS
f
plasma glucagon
plasma glucagon (pg/ml)
300
200
100
0
NS
NS
g
α-cell mass
α-cell mass (mg)
0.5
0.4
0.3
0.2
0.1
0
NS
NS
h
δ-cell mass
δ-cell mass (mg)
0.2
0.1
0
NS
NS
i
L-Δprkar1a mice
vehicle (n=3)
insulin ip (n=3)
plasma glucose (mg/dl)
60 min post insulin ip
400
300
200
100
0
*
j
prkar1a fl/fl (n=3)
L-Δprkar1a + vehicle (n=3)
L-Δprkar1a + insulin (n=3)
mRNA level
relative to control
15
10
5
0
*
*
Kiss1
k
prkar1a fl/fl
L-Δprkar1a
kisspeptin
actin
prkar1a fl/fl
L-Δprkar1a
+veh
+insulin
kisspeptin
actin

Suppl Fig. 2

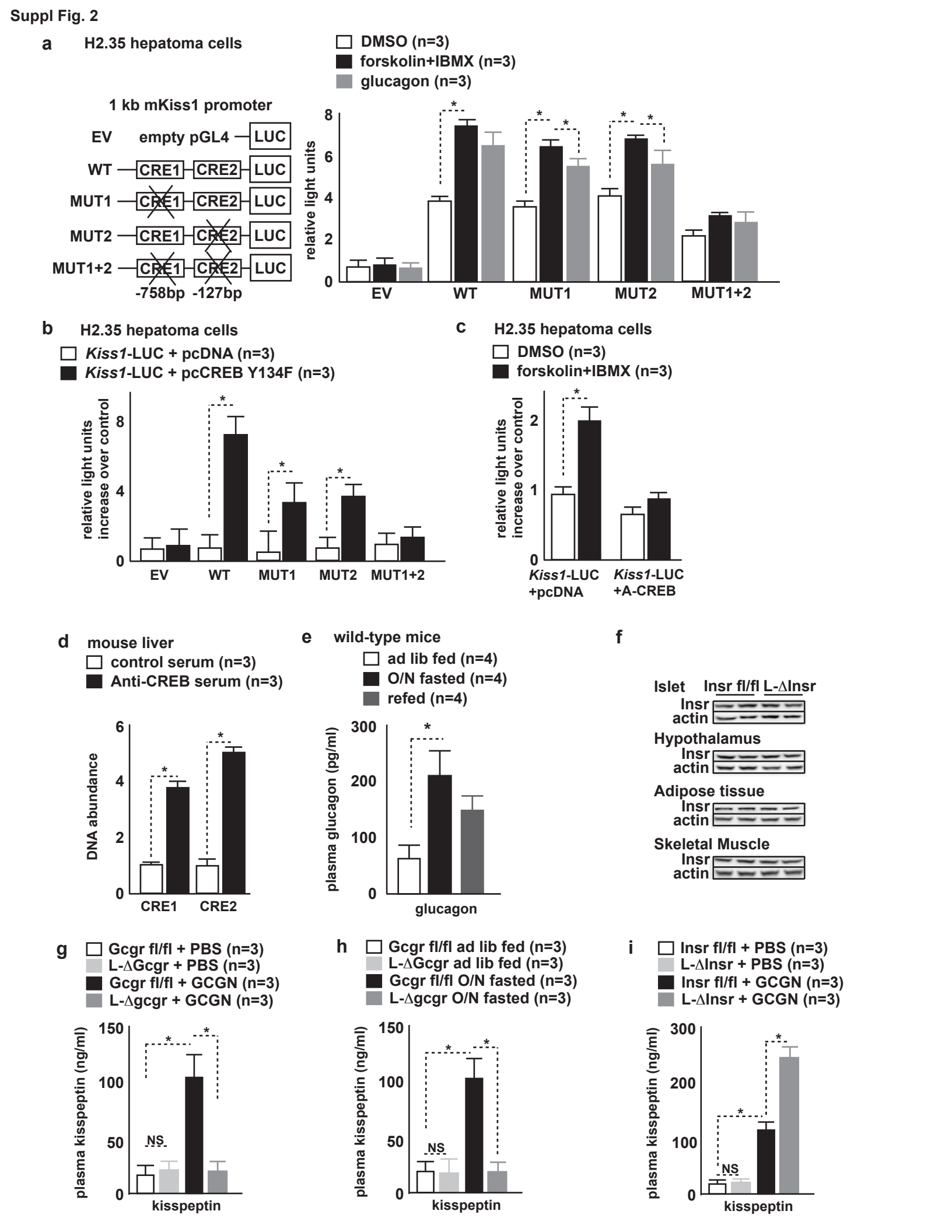
a
H2.35 hepatoma cells
DMSO (n=3)
forskolin+IBMX (n=3)
glucagon (n=3)
1 kb mKiss1 promoter
EV empty pGL4 LUC
WT CRE1 CRE2 LUC
MUT1 CRE1 CRE2 LUC
MUT2 CRE1 CRE2 LUC
MUT1+2 CRE1 CRE2 LUC
-758bp -127bp
relative light units
EV WT MUT1 MUT2 MUT1+2
b
H2.35 hepatoma cells
Kiss1-LUC + pcDNA (n=3)
Kiss1-LUC + pcCREB Y134F (n=3)
relative light units increase over control
EV WT MUT1 MUT2 MUT1+2
c
H2.35 hepatoma cells
DMSO (n=3)
forskolin+IBMX (n=3)
relative light units increase over control
Kiss1-LUC +pcDNA
Kiss1-LUC +A-CREB
d
mouse liver
control serum (n=3)
Anti-CREB serum (n=3)
DNA abundance
CRE1 CRE2
e
wild-type mice
ad lib fed (n=4)
O/N fasted (n=4)
refed (n=4)
plasma glucagon (pg/ml)
glucagon
f
Islet Insr fl/fl L-ΔInsr
Insr
actin
Hypothalamus
Adipose tissue
Skeletal Muscle
g
Gcgr fl/fl + PBS (n=3)
L-ΔGcgr + PBS (n=3)
Gcgr fl/fl + GCGN (n=3)
L-Δgcgr + GCGN (n=3)
plasma kisspeptin (ng/ml)
NS
kisspeptin
h
Gcgr fl/fl ad lib fed (n=3)
L-ΔGcgr ad lib fed (n=3)
Gcgr fl/fl O/N fasted (n=3)
L-Δgcgr O/N fasted (n=3)
plasma kisspeptin (ng/ml)
NS
kisspeptin
i
Insr fl/fl + PBS (n=3)
L-ΔInsr + PBS (n=3)
Insr fl/fl + GCGN (n=3)
L-ΔInsr + GCGN (n=3)
plasma kisspeptin (ng/ml)
NS
kisspeptin

Suppl Fig. 3

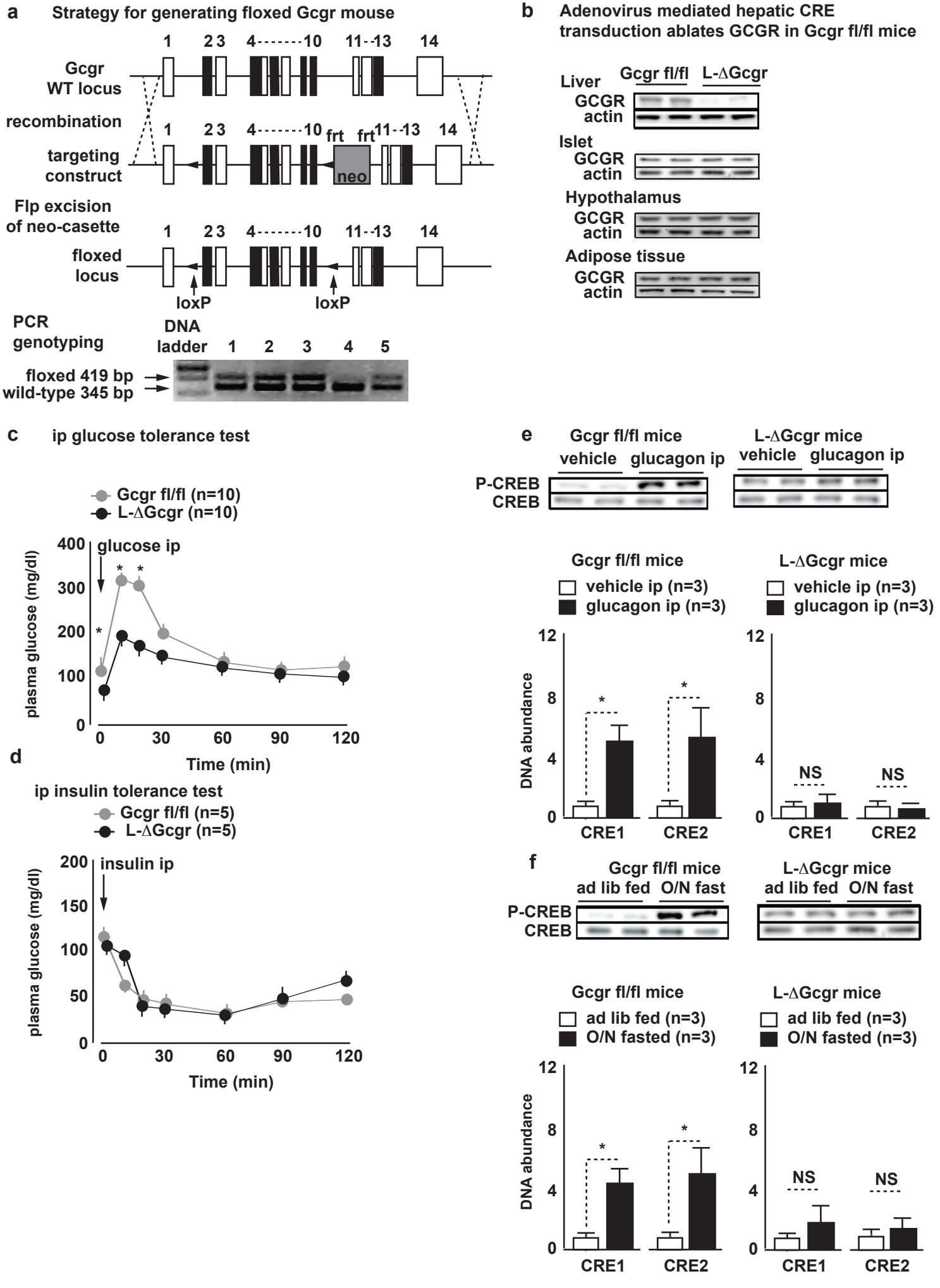
a
Strategy for generating floxed Gcgr mouse
Gcgr WT locus
recombination
targeting construct
Flp excision of neo-casette
floxed locus
loxP
loxP
frt
frt
neo
PCR genotyping
DNA ladder
floxed 419 bp
wild-type 345 bp
b
Adenovirus mediated hepatic CRE transduction ablates GCGR in Gcgr fl/fl mice
Gcgr fl/fl
L-ΔGcgr
Liver
Islet
Hypothalamus
Adipose tissue
GCGR
actin
c
ip glucose tolerance test
Gcgr fl/fl (n=10)
L-ΔGcgr (n=10)
glucose ip
plasma glucose (mg/dl)
Time (min)
d
ip insulin tolerance test
Gcgr fl/fl (n=5)
L-ΔGcgr (n=5)
insulin ip
plasma glucose (mg/dl)
Time (min)
e
Gcgr fl/fl mice
L-ΔGcgr mice
vehicle
glucagon ip
P-CREB
CREB
vehicle ip (n=3)
glucagon ip (n=3)
DNA abundance
CRE1
CRE2
NS
f
ad lib fed
O/N fast
ad lib fed (n=3)
O/N fasted (n=3)

Suppl Fig. 4

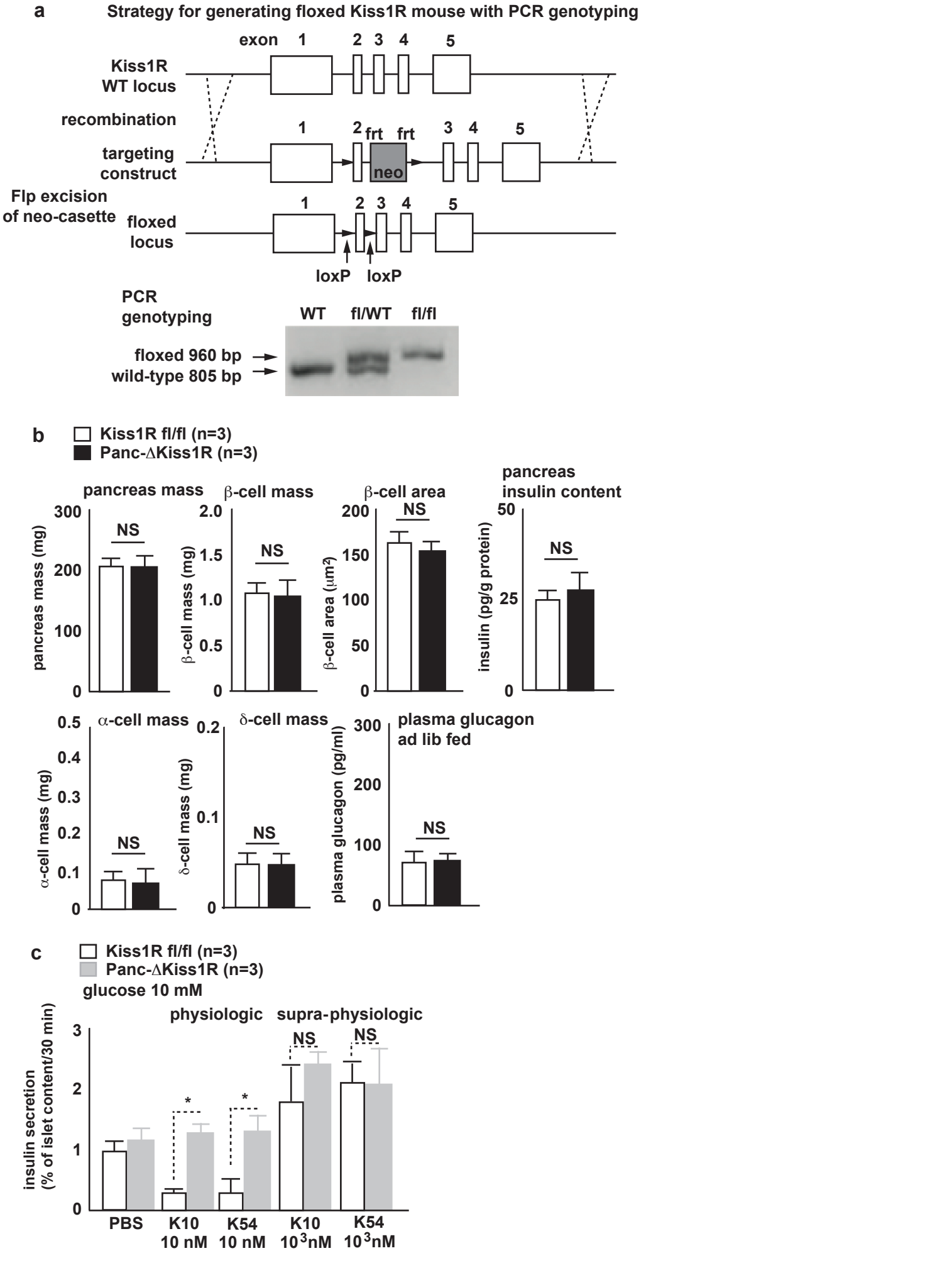
a
Strategy for generating floxed Kiss1R mouse with PCR genotyping
exon 1 2 3 4 5
Kiss1R WT locus
recombination
1 2 frt frt 3 4 5
targeting construct
neo
Flp excision of neo-casette
1 2 3 4 5
floxed locus
loxP loxP
PCR genotyping
WT fl/WT fl/fl
floxed 960 bp
wild-type 805 bp
b
Kiss1R fl/fl (n=3)
Panc-ΔKiss1R (n=3)
pancreas mass
pancreas mass (mg)
β-cell mass
β-cell mass (mg)
β-cell area
β-cell area (μm²)
pancreas insulin content
insulin (pg/g protein)
NS
α-cell mass
α-cell mass (mg)
δ-cell mass
δ-cell mass (mg)
plasma glucagon ad lib fed
plasma glucagon (pg/ml)
c
Kiss1R fl/fl (n=3)
Panc-ΔKiss1R (n=3)
glucose 10 mM
physiologic
supra-physiologic
insulin secretion (% of islet content/30 min)
*
NS
PBS
K10 10 nM
K54 10 nM
K10 10³nM
K54 10³nM

Suppl Fig. 5

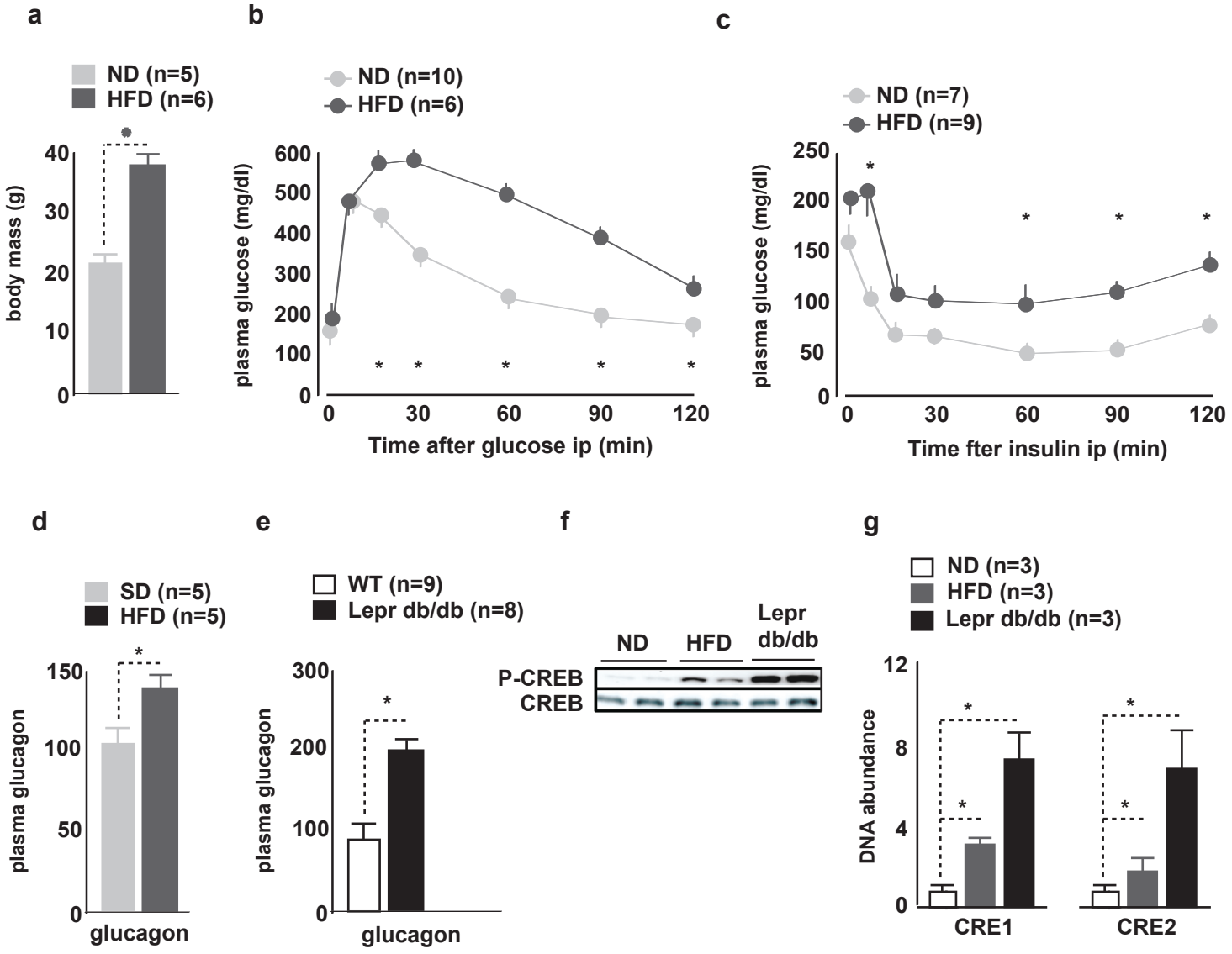
a
ND (n=5)
HFD (n=6)
body mass (g)
0
10
20
30
40
*
b
ND (n=10)
HFD (n=6)
plasma glucose (mg/dl)
0
100
200
300
400
500
600
0
30
60
90
120
Time after glucose ip (min)
c
ND (n=7)
HFD (n=9)
plasma glucose (mg/dl)
0
50
100
150
200
250
0
30
60
90
120
Time fter insulin ip (min)
d
SD (n=5)
HFD (n=5)
plasma glucagon
0
50
100
150
glucagon
e
WT (n=9)
Lepr db/db (n=8)
plasma glucagon
0
100
200
300
glucagon
f
ND
HFD
Lepr db/db
P-CREB
CREB
g
ND (n=3)
HFD (n=3)
Lepr db/db (n=3)
DNA abundance
0
4
8
12
CRE1
CRE2

Suppl Fig 6

HFD fed mice

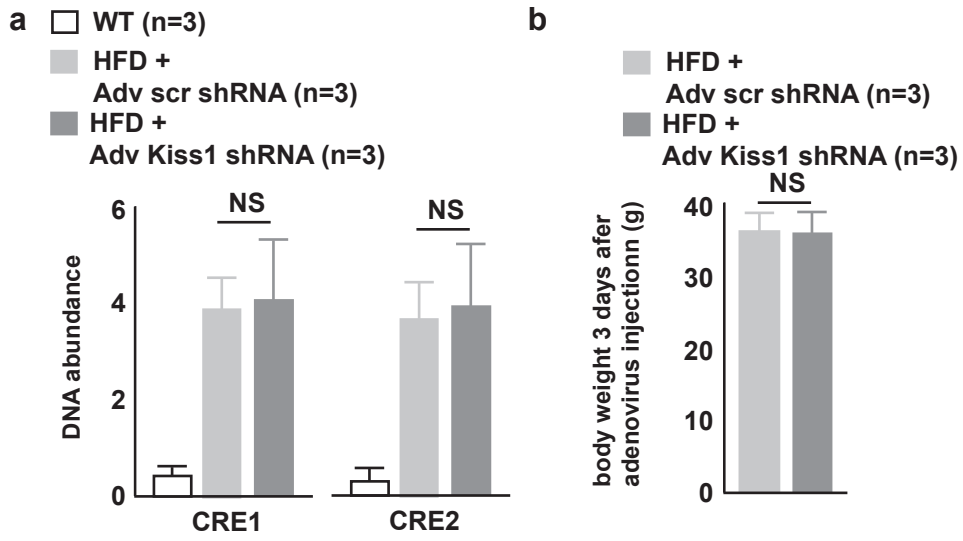

Lepr db/db mice

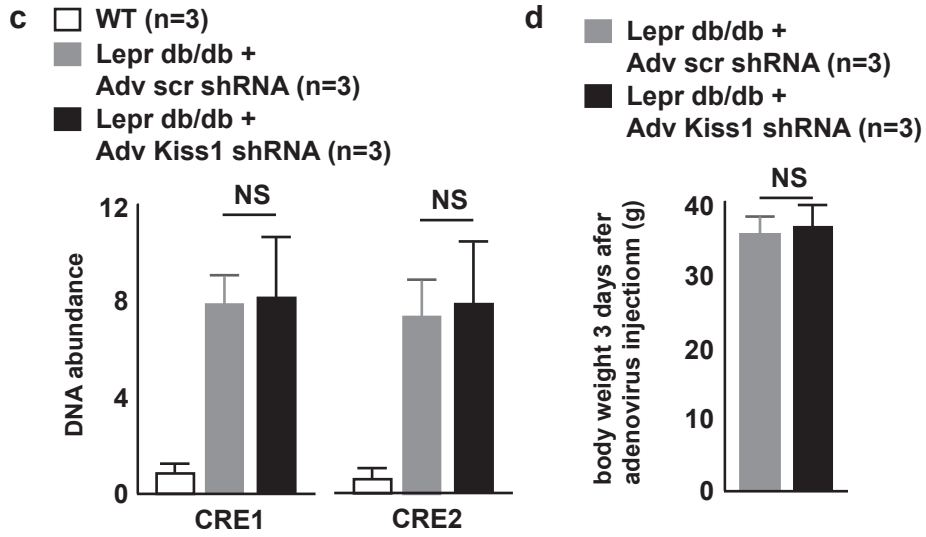

Suppl Fig 7

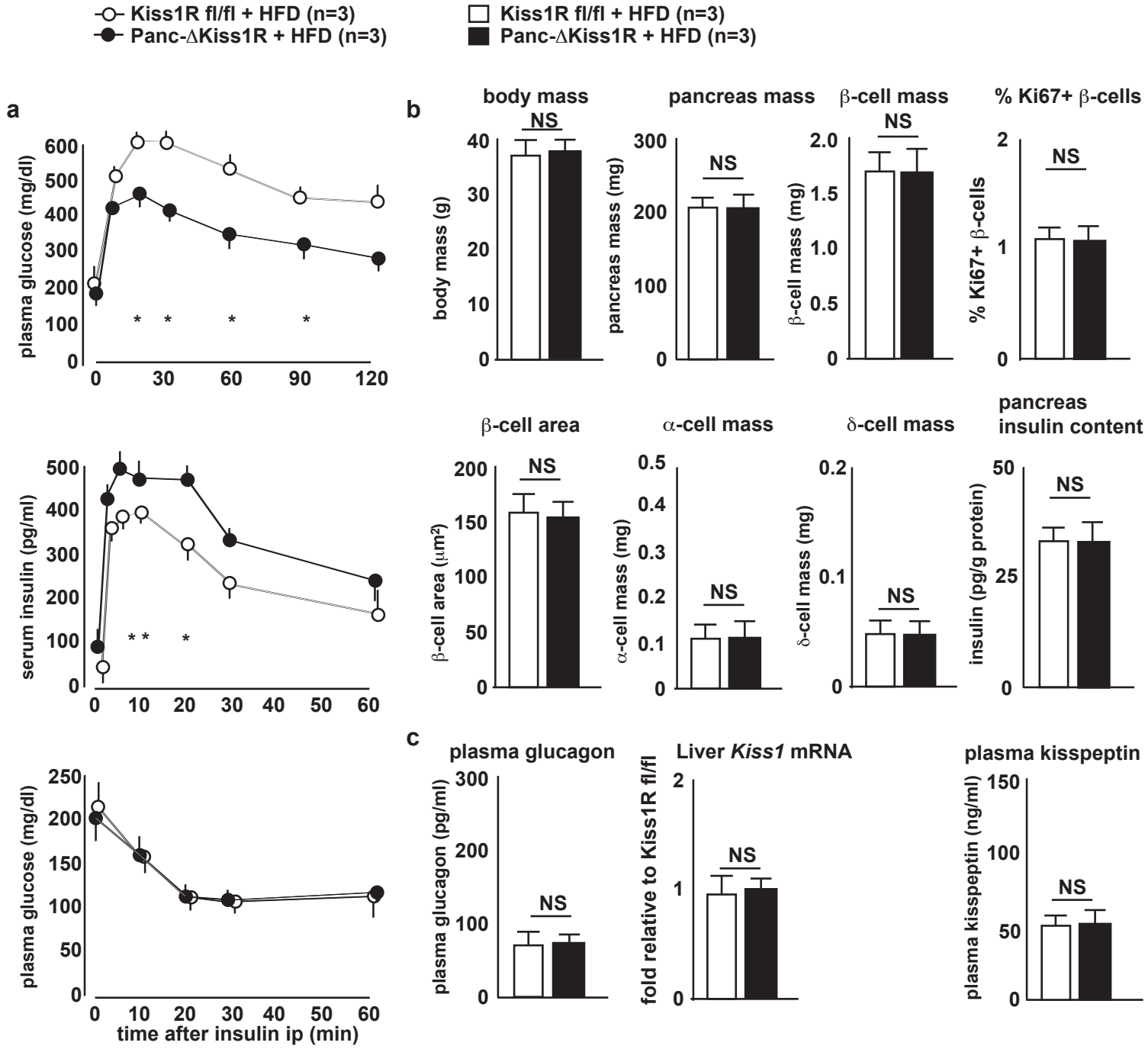
Kiss1R fl/fl + HFD (n=3)
Panc-ΔKiss1R + HFD (n=3)
Kiss1R fl/fl + HFD (n=3)
Panc-ΔKiss1R + HFD (n=3)
a
plasma glucose (mg/dl)
time after insulin ip (min)
serum insulin (pg/ml)
b
body mass
body mass (g)
pancreas mass
pancreas mass (mg)
β-cell mass
β-cell mass (mg)
% Ki67+ β-cells
% Ki67+ β-cells
β-cell area
β-cell area (μm²)
α-cell mass
α-cell mass (mg)
δ-cell mass
δ-cell mass (mg)
pancreas insulin content
insulin (pg/g protein)
NS
c
plasma glucagon
plasma glucagon (pg/ml)
Liver Kiss1 mRNA
fold relative to Kiss1R fl/fl
plasma kisspeptin
plasma kisspeptin (ng/ml)

Supplemental Figure Legends

Figure S1, related to Figure 1

Pancreas morphometric parameters and plasma glucagon levels are similar in *prkar1a*$^{fl/fl}$ and saline-infused as well as in L-Δprkar1a and D-glucose infused mice (A-G)

Panels show
A Representative IB of prkar1a in islets, hypothalamus, adipose tissue and skeletal muscle in *prkar1a*$^{fl/fl}$ and L-Δprkar1a. Actin IB is shown for protein loading control,
B Pancreas mass, **C** β-cell mass, **D** individual β-cell area, **E** Percent Ki67 positive β-cells, **F** plasma glucagon levels, **G** α-cell mass, and **H** δ-cell mass, respectively in prkar1a$^{fl/fl}$ and saline-infused as well as in L-Δprkar1a and D-glucose infused mice.

A: Adv-CRE treatment does affect prkar1a expression outside of the liver (see also **Fig. 1A**)
B-G:
β-cell proliferation is increased in L-Δprkar1a 4 days after receiving Adv-CRE treatment as compared to *prkar1a*$^{fl/fl}$ mice; and β-cell proliferation is similarly increased in mice receiving 4 days of D-glucose infusions as compared to saline-infused mice. All other parameters are similar in all groups of mice (mean±SEM, *p<0.05)

Insulin treatment in L-Δprkar1a mice downregulates liver kisspeptin1 expression (I-K)

I Plasma glucose levels 60 min after insulin treatment (1 IU/kg ip) in L-Δprkar1a mice. L-Δprkar1a mice repond to a large dose of insulin with reduction in plasma glucose at 60 min after insulin treatment (mean±SEM, *p<0.05).

J qRT-PCR of *Kiss1* in liver tissue of *prkar1a*$^{fl/fl}$ mice and in L-ΔPrkar1a mice 60 min after treatment with vehicle (PBS) or insulin (1 IU/kg ip). *Kiss1* expression is upregulated in L-ΔPrkar1a as compared to prkar1a$^{fl/fl}$ mice. Insulin treatment donwregulates *Kiss1* expression in L-ΔPrkar1a (mean±SEM, *p<0.05).

K Representative liver IB of kisspeptin **(top)** of *prkar1a*$^{fl/fl}$ and L-ΔPrkar1a mice in the fed state; **(bottom)** of prkar1a$^{fl/fl}$ mice and of L-ΔPrkar1a mice 60 min after treatment with vehicle (PBS) or insulin (1 IU/kg ip). L-ΔPrkar1a mouse livers exhibit elevated kisspeptin immunoreactivity, which is downregulated by insulin treatment.

Figure S2 related to Figure 2

Glucagon stimulates liver *Kiss1* expression via cAMP-PKA-CREB signaling

A (left) Schematic of luciferase reporter construct containing 1 kb of the murine *Kiss1* promoter with mutations in CRE1, CRE2 or both CRE1 and 2 half sites. **(right**) Relative light units indicating luciferase activity after transient transfection into H2.35 hepatoma cells of Kiss1 promoter-luciferase reporter constructs followed by treatment with forskolin (fsk) and IBMX (100 μM each). Both CRE1 and CRE2 within the *Kiss1* promoter functionally repond to frks/IBMX treatment. Mutation of both CRE1 and 2 abolishes reponse of *Kiss1* promoter to fsk/IBMX stimulation (mean±SEM, * $p<0.05$).

B Transient co-transfection in H2.35 hepatoma cells of *Kiss1* promoteer – luciferase reporter together with either empty pcDNA vector or consitutivel acvtive CREB Y134F. Both CRE1 and CRE2 within the *Kiss1* promoter respond to activation by CREB Y134F. Mutation of both CRE1 and 2 abolishes response of *Kiss1* promoter to CREB Y134F activation. (mean±SEM, * $p<0.05$).

C Transient co-transfetion in H2.35 hepatoma cells of *Kiss1* promoter – luciferase reporter together with either empty pcDNA vector or dominant negative A-CREB. Stimulation with fsk/IBMX (100 μM each) of the Kiss1 promoter luciferase reporter is abolished by co-transfection of A-CREB (mean±SEM, *$p<0.05$).

D Chromatin immunoprecipitation followed by qPCR to detect *in vivo* CREB occupancy on CRE1 and CRE2 half-sites within the *Kiss1* promoter in liver samples of WT mice using control and CREB-specific antiserum. CREB occupies both CRE1 and CRE2 within the Kiss1 promoter (mean±SEM, * $p<0.05$).

E Plasma glucagon levels in WT mice with unrestricted access to chow (ad lib fed), after an overnight fast (O/N fasted) and after regaining unrestricted access for 4 hours following an O/N fast. Plasma glucagon levels are elevated after O/N fasting and are reduced after 4 hours of refeeding (mean±SEM, * $p<0.05$).

F Representative IB in islet, hypothalamus, adipose tissue and skeletal muscle in Insr fl/fl and L-ΔInsr mice. Adv-CRE treatment does not ablate Insr in these tissues (see also **Fig. 2M**). Actin IB is shown for protein loading control.

G Plasma kisspeptin concentrations in $Gcgr^{fl/fl}$ and L-ΔGcgr mice after ip treatment with PBS or glucagon. Glucagon does not stimulate plasma kisspeptin in L-ΔGcgr mice (mean±SEM, * $p<0.05$).

H Plasma kisspeptin concentrations in $Gcgr^{fl/fl}$ and L-ΔGcgr mice in fed and fasted states. Fasting does not stimulate plasma kisspeptin in L-ΔGcgr mice (mean±SEM, * $p<0.05$).

I Plasma kisspeptin concentrations in *Insr*$^{fl/fl}$ and L-ΔInsr mice after ip treatment with PBS or glucagon. L-ΔInsr mice show a pronounced stimulation by glucagon in plasma kisspeptin (mean±SEM, * $p<0.05$).

Figure S3, related to Figures 3 and 2

Generation of Gcgr$^{fl/fl}$ mice using homologous recombination technology.

Selective adenovirus-CRE recombinase mediated liver ablation of Gcgr results in improved glucose tolerance, reduced liver CREB phosphorylation in response to glucagon treatment or overnight fasting and defective increase in CREB occupancy on the Kiss1 promoter CREB response elements (CRE) 1 and 2

A (top) Schematic depicting Grgr WT locus, the targeting construct used for homologous recombination, the resulting floxed locus and **(bottom)** PCR genotyping for WT and floxed alleles. LoxP sites were inserted flanking exons 2 through 10. PCR genotyping differentiates WT and floxed alleles.

B Representative IB for glucagon receptor (GCGR) in *Gcgr$^{fl/fl}$* mice three days after treatment with Adv-GFP or Adv-CRE to ablate liver glucagon receptor expression (L-ΔGcgr mice). GCGR is efficiently ablated *in vivo* in liver tissue of L-ΔGcgr mice while GCGR remains detectable in control *Gcgr$^{fl/fl}$* mice. Adv-CRE treatment does not ablate GCGR in islets, hypothalamus, adipose tissue. Actin IB is shown for loading control.

C Plasma glucose levels during **(top)** ip GTT and **(bottom)** during ip ITT in *Gcgr$^{fl/fl}$* and L-ΔGcgr mice. L-ΔGcgr mice exhibit improved glucose tolerance and similar insulin tolerance as compared to Gcgr fl/fl mice (mean±SEM).

D (top) Representative liver IB showing pCREB and total CREB in liver 60 minutes after glucagon (100 μg/kg ip) treatment in Gcgr and L-ΔGcgr mice. CREB phosphorylation is stimulated in *Gcgr$^{fl/fl}$* control mice, but is significantly reduced in mice lacking liver glucagon receptor (L-ΔGcgr mice); **(bottom)** Chromatin immunoprecipitation followed by qPCR to detect *in vivo* CREB occupancy on CRE1 and CRE2 half-sites within the *Kiss1* promoter in liver 60 minutes after glucagon (100 μg/kg ip) treatment in Gcgr and L-ΔGcgr mice. CREB occupancy of CRE1 and CRE2 of the Kiss1 promoter increases after glucagon treatment in *Gcgr$^{fl/fl}$* but not in L-ΔGcgr mice (mean±SEM, * $p<0.05$).

E (top) Representative liver IB extracts showing pCREB and total CREB in liver of *Gcgr$^{fl/fl}$* and L-ΔGcgr mice with unrestricted accss to chow (ad lib fed) or after an overnight fast (O/N fasted). CREB phosphorylation is stimulated in *Gcgr$^{fl/fl}$* control mice, but is significantly reduced in mice lacking liver glucagon receptor (L-ΔGcgr mice); **(bottom)** Chromatin immunoprecipitation followed by qPCR to detect *in vivo* CREB occupancy on CRE1 and CRE2 half-sites within the *Kiss1* promoter in liver of *Gcgr$^{fl/fl}$* and L-ΔGcgr mice with unrestricted accss to chow (ad lib fed) or after an overnight fast (O/N fasted). CREB occupancy of CRE1 and CRE2 of the Kiss1 promoter increases after an overnight fast in *Gcgr$^{fl/fl}$* but not in L-ΔGcgr mice (mean±SEM, * $p<0.05$).

Figure S4, related to Figure 4

Generation of Kiss1R$^{fl/fl}$ mice using homologous recombination technology. Pancreas Kiss1R ablation does not affect pancreas morphometric parameters. Kisspeptin at nanomolar concentrations suppresses glucose stimulated insulin secretion from cultured islets in a Kiss1R-dependent manner

A (top) Schematic depicting Kiss1R WT locus, the targeting construct used for homologous recombination, the resulting floxed locus and **(bottom)** PCR genotyping for WT and floxed alleles. LoxP sites were inserted flanking exon 2. PCR genotyping differentiates WT and floxed alleles.

B Panels show
Pancreas mass, β-cell mass, individual β-cell area, pancrease insulin content, α-cell mass, δ-cell mass, and plasma glucagon levels in the fed state, respectively in Kiss1R fl/fl and in Panc-ΔKiss1R mice. *Kiss1R$^{fl/fl}$* and Panc-ΔKiss1R do not differ in pancreas morphometric parameters, insulin content or plasma glucagon levels (mean±SEM).

C Glucose-stimulated insulin secretion during static incubation in 10 mM glucose of islets from *Kiss1R$^{fl/fl}$* and Panc-ΔKiss1R mice in response to vehicle (PBS) and to physiologic (10 nM) and supraphysiologic (10^3 nM) kisspeptin 10 (K10) concentrations (mean±SEM, * $p<0.05$). Physiologic K10 concentrations inhibit GSIS from *Kiss1R$^{fl/fl}$* and Panc-ΔKiss1R islets are resistant to K10 mediated GSIS suppression. At unusually high suprapysiologic K10 concentrations K10 stimulates GSIS in a Kiss1R-independent manner in both *Kiss1R$^{fl/fl}$* and Panc-ΔKiss1R islets.

Figure S5, related to Figure 5

High fat diet fed mice and *Lepr*$^{db/db}$ mice exhibit increased plasma glucagon levels, increased liver CREB phosphorylation and *in vivo* liver CREB occupancy of CRE1 and 2 within the Kiss1 promoter.

A Body mass of male littermate mice after receiving for 8 weeks standard diet (SD) and high fat diet (HFD). HFD causes an increase in body weight (mean±SEM, * p<0.05).

B Plasma glucose levels during **(left)** ip GTT and **(right)** during ip ITT in male mice after receiving for 8 weeks standard diet (SD) and high fat diet (HFD). HFD fed mice exhibit impaired glucose tolerance as well as reduced insulin tolerance (mean±SEM, * p<0.05).

C Plasma glucagon levels in the fed state in male mice after receiving for 8 weeks standard diet (SD) and high fat diet (HFD). HFD fed mice exhibit elevated plasma glucagon levels as compared to mice kept on SD (mean±SEM, * p<0.05)

D Plasma glucagon levels in the fed state in 3-4 week old male WT mice and in age-matched male db/db mice. *Lepr*$^{db/db}$ mice exhibit elevated plasma glucagon levels as compared to WT mice (mean±SEM, * p<0.05).

E Representative liver of pCREB and total CREB of WT mice kept on SD, in mice recieiving 8 weeks of HFD and 3-4 week old male *Lepr*$^{db/db}$ mice. HFD fed mice and *Lepr*$^{db/db}$ mice show increased pCREB. Db/db mice show higher CREB phosphorylation status than HFD fed mice (mean±SEM).

F Chromatin immunoprecipitation followed by qPCR to detect *in vivo* CREB occupancy on CRE1 and CRE2 half-sites within the *Kiss1* promoter in liver samples of WT mice kept on SD, in mice recieiving 8 weeks of HFD and 3-4 week old male *Lepr*$^{db/db}$ mice. HFD fed and *Lepr*$^{db/db}$ mice show increased CREB occupancy of both CRE1 and 2 half-sites within the Kiss1 promoter (mean±SEM, * p<0.05).

Figure S6, related to Figure 6

In HFD fed and *Lepr*$^{db/db}$ mice shRNA-mediated *Kiss1* knockdown does not alter *in vivo* CREB occupancy of CRE1 and 2 half-sites in *Kiss1* promoter.
shRNA-mediated *Kiss1* knockdown as compared to scrambled shRNA treamtnet does not change body weight in HFD fed mice or *Lepr*$^{db/db}$ mice.

HFD fed mice

A Chromatin immunoprecipitation followed by qPCR to detect *in vivo* CREB occupancy on CRE1 and CRE2 half-sites within the *Kiss1* promoter in liver samples from control mice kept on a standard diet (SD) and mice kept for 8 weeks on a HFD before treatment with Adv Kiss1–shRNA or control adenovirus scr-shRNA. Liver tissue was collected 3 days after adenovirus treatment. CREB occupancy on Kiss1 CRE half sites 1 and 2 in HFD fed mouse liver is increased as compared to liver from SD fed mice. Adenovirus mediated Kiss1 knockdown in HFD fed mice does not affect CREB occupancy of CRE 1 and 2 half-sites in the Kiss1 promoter (mean±SEM, * $p<0.05$).

B Body weight in HFD fed mice 3 days after treatment with Adv-scr shRNA or Adv-Kiss1 shRNA. Body weight is similar in HFD fed mice and unaffected by Adv treatment (mean±SEM).

Lepr db/db mice

C Chromatin immunoprecipitation followed by qPCR to detect *in vivo* CREB occupancy on CRE1 and CRE2 half-sites within the *Kiss1* promoter in liver samples from control WT and 4-5 week old *Lepr*$^{db/db}$ mice before treatment with Adv Kiss1–shRNA or control adenovirus scr-shRNA. Liver tissue was collected 3 days after adenovirus treatment. CREB occupancy on Kiss1 CRE half sites 1 and 2 in *Lepr*$^{db/db}$ mouse liver is increased as compared to liver from WT mice. Adenovirus mediated Kiss1 knockdown in *Lepr*$^{db/db}$ mice does not affect CREB occupancy of CRE 1 and 2 half-sites in the Kiss1 promoter (mean±SEM, * $p<0.05$).

D Body weight in 4-5 week old Lepr db/db mice 3 days after treatment with Adv-scr shRNA or Adv-Kiss1 shRNA. Body weight is similar in L-Δprkar1a mice and unaffected by Adv treatment (mean±SEM).

Figure S7, related to Figure 7

High fat diet fed mice lacking pancreas Kiss1R have improved glucose tolerance owing to increased glucose stimulated insulin secretion

A (top) plasma glucose, **(middle)** serum insulin during ip GTT and **(bottom**) plasma glucose during ipITT in 14 week old male *Kiss1R*$^{fl/fl}$ mice and Panc-ΔKiss1R mice after receiving 8 weeks of HFD. Panc-ΔKiss1R mice have improved glucose tolerance as compared to *Kiss1R*$^{fl/fl}$ counterparts. Insulin resistance as reflected by similar ITT is similar in *Kiss1R*$^{fl/fl}$ and Panc-ΔKiss1R mice (mean±SEM).

B Pancreas morphometry in 14 week old male *Kiss1R*$^{fl/fl}$ mice and Panc-ΔKiss1R mice receiving after 8 weeks of HFD. Body mass, pancreas mass, β-cell mass and –size, % Ki67 positive β-cell reflecting β-cell proliferation activity, α-cell mass, δ-cell mass and pancreas insulin content are similar in Kiss1R$^{fl/fl}$ mice and Panc-ΔKiss1R mice (mean±SEM).

C Plasma glucagon, liver *Kiss1* mRNA levels and plasma kisspeptin levels are similar in 14 week old male *Kiss1R*$^{fl/fl}$ mice and Panc-ΔKiss1R mice receiving after 8 weeks of HFD (mean±SEM, * $p<0.05$)

Experimental procedures.

Animals

Generation of *Gcgr*$^{fl/fl}$ and *Kiss1R*$^{fl/fl}$ mice. *Gcgr*$^{fl/fl}$ were generated together with Ingenious Targeting Laboratories. A targeting construct for mouse Gcgr was generated by bacterial recombineering with a loxP sequence inserted upstream of the second exon. A second loxP containing cassette including neomycin resistance separately flanked by FLPe (FRT) recognition sequences (Rodriguez et al., 2000) inserted downstream of exon 10. Location of LoxP sites predicted after CRE-mediated recombination lack of any protein product to be generated (**Fig. S3**). To generate *Kiss1R*$^{fl/fl}$ mice, a targeting construct was created as described (Na et al., 2013) and contained a loxP site upstream of the second exon and one loxP containing cassette including neomycin resistance separately flanked by FLPe (FRT) recognition sequences 3' of the second exon. Location of LoxP sites predicted after CRE-mediated recombination lack of the second transmembrane domain of Kiss1R (**Fig. S4**). The reproductive deficiency of gonadotrope-specific CRE-mediated Kiss1R ablation in *Kiss1R*$^{fl/fl}$ mice has been separately reported (Novaira et al., 2013). Homologous recombination of targeting constructs in embryonic stem cells was achieved as described (Mortensen, 2006). Proper insertion was ascertained by PCR screening as well as Southern blot. Chimerae were generated after C57Bl/6 blastocyst injection and embryonic propagation in pseudo-pregnant females. Germline transmission was confirmed by PCR genotyping tail DNA extracts. The first offspring was interbred with Actin-FLPe deleter mice (Jackson Laboratories) (Rodriguez et al., 2000) to eliminate the neomycin cassette. Both *Gcgr*$^{fl/fl}$ and *Kissr*$^{fl/fl}$ mice were viable, fertile, transmitted the modified gene in Mendelian pattern and showed no obvious defects in body weight or metabolism. Mice were backcrossed at least 6 times into C57Bl/6 background. Primers used for genotyping mice are provided below.

Primers used for PCR genotyping mice

Prkar1a fl/fl	FW	GCA GGC GAG CTA TTA GTT TA
	RV	CAT CCA TCT CCT ATC CCC TTT
Kiss1R fl/fl	FW	TTC GTG AAC TAC ATC CAG CAG
	RV	AGA GTG GCA CAT GTG GCT TG
Gcgr fl/fl	FW	TCA CCC GTG ATG ATC CCA TGT CTT
	RV	AGT GGC TCA CAG TGC CTA TTC AGA
Insr fl/fl	FW	GAT GTG CAC CCC ATG TCT G
	RV	CTG AAT AGC TGA GAC CAC AG
Lepr db/db	FW	AGA ACG GAC ACT CTT TGA AGT CTC
	RV	CAT TCA AAC CAT AGT TTA GGT TTG T
		restriction enzyme digestion (RsaI) after PCR

To generate HFD fed glucose intolerant animals, 6-week old C57Bl/6J male mice were fed for 8 weeks a diet containing 60% calories as lipids (Bioserv). Controls were male littermates fed regular diet in parallel.

For overnight fasting, animals were restricted access to food overnight from 6pm until 9 am (=O/N fasted). A subset of mice was refed by allowing unrestricted access to food after overnight fasting for 4 hours before analysis (refed). Mice without any restriction to food (=ad lib fed) were allowed unrestricted acces to food at all times.

Intraperitoneal glucose tolerance (ipGTT) and insulin tolerance (ipITT) tests were performed according to standard protocols (Song et al., 2013; Song et al., 2011). After 9 am – 3 pm fasting, animals were administered 20% D-glucose (via ip injection), insulin 0.5 U/kg i.p. (Novolin), glucagon (100 μg/kg i.p. (Sigma)). K54 (Gly-Thr-Ser-Leu-Ser-Pro-Pro-Pro-Glu-Ser-Ser-Gly-Ser-Arg-Gln-Gln-Pro-Gly-Leu-Ser-Ala-Pro-His-Ser-Arg-Gln-Ile-Pro-Ala-Pro-Gln-Gly-Ala-Val-Leu-Val-Gln-Arg-Glu-Lys-Asp-Leu-Pro-Asn-Tyr-Asn-Trp-Asn-Ser-Phe-Gly-Leu-Arg-Phe-NH_2, 10 nmol; Calbiochem), or K10 (Tyr-Asn-Trp-Asn-Ser-Phe-Gly-Leu-Arg-Phe-NH_2, 10 nmol; Calbiochem) was administered simultaneously with glucose during ipGTT. The glucagon receptor antagonist GAI (N-(3-Cyano-6-(1,1-dimethylpropyl)-4,5,6,7-tetrahydro-1-benzothien-2-yl)-2-ethylbutanamide

(Qureshi et al., 2004) and its non-active analogue were administered (50 mg/kg i.p. in DMSO) in HFD fed and *Lepr*$^{db/db}$ mice 60 min before i.p.GTT. Intraperitoneal pyruvate converstion (1g/kg i.p.) test (ipPCT) in ΔL-Prkar1a mice was performed in the fed state (9 am) to avoid any confounding effects of fasting-induced elevated endogenous glucagon levels. Tail-vein blood was collected at the indicated times in figures for glucose and insulin measurements. Serum insulin was measured using mouse magnetic bead panel (Millipore, Luminex). Plasma for glucagon measurements was drawn from mice in the fed state at 9 am, unless otherwise noted for fasting studies. Plasma glucagon (Alpco) and kisspeptin1 (USCN Life Sciences Inc E92559Ra) were measured by ELISA according to manufacturers instructions including dilution of samples. Because kisspeptin1 ELISA detects K10 and does not differentiate between the various bioactive kisspeptin1 breakdown products, the plasma concentrations measured with ELISA are provided according to manufacturers' instructions and were not converted into SI units.

All animal studies were performed at least in triplicate. For studies involving standard (Taconic) and high fat diet (60% calories from saturated fat; Bioserv) care was taken to assign littermates to different diets and to perform tests in age matched animals. Animals were randomized to different treatments described herein. Replicates were obtained testing different individual animals and not by repeat testing the same animal. Animal tests and sample measurements (e.g. ELISA) from animal tests were performed in a blinded manner.

Adenovirus (Adv-CRE and Adv-GFP, University of Iowa Genetics Core) were injected into tail vein (10^9 plaque forming units/mouse in 1xPBS). Adv-CRE injection into mice carrying a floxed stop codons upstream of YFP at the Rosa26 locus (Jackson Laboratories) showed 95% of hepatocytes are transduced with CRE recombinase. Occasional recombination was found in lung tissue but not in brain, heart, kidney, pancreas, islet, spleen, muscle confirming strong liver targeting by injected adenovirus (not shown). Immunoblots of islets, hypothalamus, adipose tissue, and skeletal muscle in L-Δprkar1a, L-ΔGcgr, L-ΔInsr mice confirmed that, Prkar1a, Gcgr, and Insr were

expressed at unchanged levels relative to control (Adv-GFP treated counterparts) and that corresponding floxed genes had not been ablated in these tissues by Adv-CRE treatment.

***In vivo* cannulation and perfusion.**

For catheterization, mice were anesthetized with inhaled 2% isoflurane. Micro-renathane catheters (Braintree Scientific) were inserted in the left femoral artery and vein, sutured in place, stabilized with superglue (Henkel), tunneled subcutaneously to the upper back by threading through a blunt needle, taped to a wire attached to posterior cervical muscles for stiffness (A-M-Systems), and connected to a 360° dual channel swivel designed for mice (Instech, Plymouth Meeting). Mice received infusions of 0.9% sodium chloride or 50% dextrose. Detailed protocols are provided in reference (Alonso et al., 2007).

Immunohistochemistry and pancreas morphometrical analysis.

At least 3 Bouin's-fixed and paraffin embedded pancreas sections/mouse 150 μM apart were immuno-stained and analyzed for islet/β-, α- and δ-cell mass as described (Song et al., 2011). Confocal imaging was performed on a fluorescence microscope (Zeiss) equipped with confocal and digital image capturing capabilities.

Gene expression analysis.

Microarray expression profiles were generated using the Illumina MouseRef-8 v2 BeadChips (Illumina, San Diego, CA) by the Genome Sciences Laboratory at the University of Virginia. Biotin-labeled cRNA was synthesized by the total prep RNA amplification kit from Ambion (Austin, TX). cRNA was quantified and normalized to 150 ng/ul, and then 750 ng was hybridized to each BeadChip. The image data was then acquired by scanning the chips on an Illumina iScan. The raw idat files were uploaded into the Illumina Genomestudio software and the data exported for analysis. Sample and control probe signal intensities were exported from GenomeStudio. These files were imported into R version 2.15.0, quantile normalized, and log2 transformed using the Bioconductor beadarray package, version 2.6.0, and Illumina probe IDs were

annotated using the Bioconductor illuminaMousev2.db package, version 1.16.0. The BioConductor array QualityMetrics package, version 3.12.0 was used to perform quality assessment. For examining differential gene expression, a linear model was with empirical-Bayes moderated standard errors using the limma package, version 3.14.11. Gene-set enrichment analysis (GSEA) was used to examine differential expression results for enriched pathways (Smyth, 2004; Subramanian et al., 2005). SignalP 4.0 was used with the default parameters to determine which differentially expressed genes contained a cellular export signal based on the amino acid sequence (Petersen et al., 2011). A cut-off for False discovery rate-corrected P<0.05 and log2 Fold Change (FC)≥2 was used to identify a significant change in gene expression. Array results of interest were validated by quantitative RT-PCR (qRT-PCR).

RT-PCR

RNA was isolated using Illustra RNAspin combined with removal of DNA by DNAseI digestion (GE Healthcare). QPCR was carried out following standard procedures using SYBR green (BioRad) using mouse primers indicated in Supplemental Table1. Expression levels were calculated using the $2^{-\Delta\Delta}$CT method with 18S rRNA as internal control (Livak and Schmittgen, 2001). PCR primers are provided below.

Primers used for quantitative PCR

Kiss1	Kiss1 F	GCATACCGCGATTCCTTTT
	Kiss1 R	AGCTGCTGCTTCTCCTCTGT
Gcgr	GCGR F	TGCTGTTTGTCATCCCCTG
	GCGR R	CAGGAAGACAGGAATACGCAG
Kiss1R	Gpr54 F	GCAAATTCGTCAACTACATCCAG
	Gpr54 R	GGGAACACAGTCACATACCAG
18sRNA	18S-F	GCAATTATTCCCCATGAACG
	18S-R	GGCCTCACTAAACCATCCAA
Actin	Act F	AGCCATGTACGTAGCCATCC
	ActR	CTCTCAGCTGTGGTGGTGAA

Ppargc1a	Pgc1 F	CAGCCTCTTTGCCCAGATCT
	Pgc1 R	CCGCTAGCAAGTTTGCCTCA
Src1	Src1 F	AGGAGTGATAGAGAAGGAGTCG
	Src1 R	TGATTGTAACCCAAGTAGCTGG
Pck1	Pck1 F	CTGCATAACGGTCTGGACTTC
	Pck1 R	CAGCAACTGCCCGTACTCC
G6P	G6p F	CGACTCGCTATCTCCAAGTGA
	G6p R	GTTGAACCAGTCTCCGACCA
For ChIP assay		
Kiss1pr CRE 1	KCRE1 F	TGTCGTCTTTGGCTTCCT
	KCRE1 R	TGCACCTAGGGTAGCAC
Kiss1pr CRE2	KCRE2 F	AGGCGAGTGCCTTGAAC
	KCRE2 R	CCACTTTCTTCTGGACTTGGA

Islet studies

Islet isolation was performed by collagenase digestion, gradient centrifugation and three rounds of microscope-assisted manual picking of islets (Song et al., 2011). Static incubation studies were conducted as previously described with 20 hand-picked equal-sized islets were studied in each group. Islets were cultured in RPMI 1640 medium (Invitrogen) containing 10 or 20 mM D-glucose (as indicated) and supplemented with 0.2% bovine serum albumin, 1% each Na-Pyruvate, HEPES, Penicillin/Streptomycin. After 30 min incubation glucose concentrations, supernatant was taken for insulin measurements and pelleted islets were taken in acid ethanol (0.18M HCl in 70% ethanol) for insulin measurements in islets (Alpco). Islet protein concentration was measured using the BCA method (Thermo Fisher).

Insulin secretion during static incubation. After overnight culture (37 C, 5% CO2, 95% O2 in humid chamber) of isolated islets in RPMI 1640 (Mediatech) containing 5 mM glucose, 1% each Na-Pyruvate, HEPES, Penicillin/Streptomycin and 0.2% bovine serum albumin (BSA), islets were switched to either 10 or 20 mM glucose containing

RPMI 1640. Where indicated, Kisspeptin-10 (0-100 nM, and 1 μM), E4 (10 nM) or vehicle (PBS) was added. After 30 min incubation glucose concentrations, supernatant was taken for insulin measurements and pelleted islets were taken in acid ethanol (0.18M HCl in 70% ethanol) for insulin measurements in islets (ELISA, Alpco). Islet protein concentration was measured using the BCA method (Thermo Fisher).
Dose response curves of GSIS inhibition by Kisspeptin-54 or -10 (0-100 nM) to serve as a functional bioassay for plasma kisspeptin1 activity performed at 6 separate times provided intra-assay and inter-assay coefficient of variations of 7.3% and 9.2%, respectively.

For studies with plasma incubation, a final concentration of plasma was 1% or 10% (vol/vol). Plasma was treated with a protease inhibitor cocktail containing 4-(2-Aminoethyl) benzenesulfonyl fluoride hydrochloride (1mM), Aprotinin (0.8 μ M), bestatin (50 μM), (1S,2S)-2-(((S)-1-((4-Guanidinobutyl)amino)-4-methyl-1-oxopentan-2-yl)carbamoyl)cyclopropanecarboxylic acid (15 μM), EDTA (5 μM), leupeptin (20 μM), pepstatin A (10 μM) (Liu et al., 2013) (Thermo-Fisher), K54, K10, E4 were added at the concentrations indicated in the relevant figures. Islets were taken in 0.18M HCL/ 70% ethanol to extract and measure total islet insulin content. cAMP concentrations were measured in islet extracts using ELISA (Enzo Life Sciences).

Perifusion studies were performed as previously published (Song et al., 2013; Song et al., 2011) with slight modifications. The perifusate was Krebs ringer buffer (KRB) (37 C, pH 7.4) containing 0.2% BSA fraction V, 24 mM sodium bicarbonate and was gassed with 95% air and 5% CO2. Perifusion (1ml/min) occurred for the first 30 minutes with a KRB containing 3 mM glucose for equilibration, after which time the perifusate was collected in 1 ml fractions. After additional 10 minutes, glucose in the perifusate was increased to 10 mM. Where indicated, K10 (10 nM) or E4 (10 nM) was added to the perifusate. Insulin was measured in selected individual eluent fractions at 30, 35, 40, 42, 45, 50, 55, 60 min (Alpco ELISA). The first 10 minutes after increasing glucose was defined as first phase, the period thereafter was defined as second phase of insulin secretion. At the end of the perifusion protocol, 30mM KCL was administered into the perifusate to

depolarize β-cells. Insulin levels were normalized to total islet protein, which was spectrophotometrically determined (Eppendorf) after completion of the perifusion protocol.

Cell culture studies

Mouse primrary hepatocytes were isolated and cultured as described (He et al., 2009). H2.35 hepatoma cell line was cultured and transfected as described (He et al., 2009). 1kb of the 5' untranslated region of the mouse *Kiss1* gene were cloned by PCR into pGL4. The CRE half sites (TGCAT) within the promoter region were mutated by site directed mutagenesis to (TATGT). Luciferase activity was measured in cell lysates using a luminometer (Berthold) after treatment each for 2 hours with forskolin/IBMX (100 μM each) or glucagon (200 pg/ml) or/and insulin (2000 pg/ml). Dominant-negative A-CREB (Ahn et al., 1998) and WT CREB were from Addgene. Constituively active CREB Y134F (Du et al., 2000) was generated by site directed mutagenesisof WT CREB.

Protein Immunoblots

Immunoblots (IB) were performed with 40-50 μg protein taken in lysis buffer (Cell Signaling). Representative blots are shown. Actin IB of corresponding samples are shown for protein loading references. Chromatin immunoprecipitation studies were performed as described (Song et al., 2011). Antibodies used are listed below.

Primary antibodies used for immunoblots and immunohistochemistry.

Antibody	Vendor	Cat. No.	Fold Dilution
Mouse anti-Actin	Millipore	MAB1501	4000
Mouse anti-PKA[RI]	BD Transduction Laboratories	610165	500
Mouse anti-PKA[RIa]	BD Transduction Laboratories	610609	250
Mouse anti-PKA[RIIa]	BD Transduction Laboratories	612242	2000
Mouse anti-PKA[RIIB]	BD Transduction Laboratories	610625	2000
Mouse anti-PKA[C]	BD Transduction Laboratories	610980	2000
Rabbit anti-CREB-1	Santa Cruz	sc-58	100
Rabbit anti- Ser133-Phospho CREB	Abcam	ab30651	500
Rabbit anti Kisspeptin10	Millipore	AB9754	400
Rabbit anti-Kiss1R	Phoenix Pharmaceuticals	H-001-64	200
Rabbit anti glucagon receptor	Novus biological	NBP1-00850	400
Mouse anti-insulin receptor	Abcam	ab69508	1000
Guinea-pig anti-insulin	DAKO	A0564	1000
Rabbit anti-glucagon	Zymed	18-0064	550
Rabbit anti-somatostatin	DAKO	A0566	200

Human studies

Tests on de-identified human samples were approved by the Johns Hopkins University Institutional Review Board. Liver tissue from humans without diabetes mellitus and with T2DM were obtained from Origene and National Disease Research Interchange (NDRI). Serum samples from humans without and with T2DM were from NDRI. Samples from T2DM were from poorly controlled diabetics, not receiving insulin or metformin treatment. Details of samples are provided below.

Human liver tissue and islet information

Tissue	Source	Gender	Age	Diagnosis	Treatment	Cause of Death
Liver	NDRI OD26532	Female	65y	T2DM x 2 weeks, HTN	none	CV stroke
Liver	NDRI OD26278	Male	94y	T2DM x 31y	glipizide, lisinopril	Resp. failure
Liver	NDRI OD2072	Male	78y	T2DM untreated	none	Cardiac arrest
Liver	Origene CP565754	Not provided	Not provided	Normal, no T2DM	none	Not provided
Liver	Origene CP565527	Not provided	Not provided	Normal, no T2DM	none	Not provided
Liver	Origene CP565735	Not provided	Not provided	no T2DM	none	Not provided
Islet protein	NDRI OD18253	Female	40y	Normal, no T2DM	none	CV stroke
Islet protein	NDRI OD1860	Male	65y	Normal, no T2DM	none	CV stroke
Islet protein	NDRI OD40157	Male	27y	Normal, no T2DM	none	trauma

References to Supplemental Information

Ahn, S., Olive, M., Aggarwal, S., Krylov, D., Ginty, D.D., and Vinson, C. (1998). A dominant-negative inhibitor of CREB reveals that it is a general mediator of stimulus-dependent transcription of c-fos. Mol Cell Biol *18*, 967-977.

Alonso, L.C., Yokoe, T., Zhang, P., Scott, D.K., Kim, S.K., O'Donnell, C.P., and Garcia-Ocana, A. (2007). Glucose infusion in mice: a new model to induce beta-cell replication. Diabetes *56*, 1792-1801.

Du, K., Asahara, H., Jhala, U.S., Wagner, B.L., and Montminy, M. (2000). Characterization of a CREB gain-of-function mutant with constitutive transcriptional activity in vivo. Mol Cell Biol *20*, 4320-4327.

He, L., Sabet, A., Djedjos, S., Miller, R., Sun, X., Hussain, M.A., Radovick, S., and Wondisford, F.E. (2009). Metformin and insulin suppress hepatic gluconeogenesis through phosphorylation of CREB binding protein. Cell *137*, 635-646.

Liu, Z., Ren, C., Jones, W., Chen, P., Seminara, S.B., Chan, Y.M., Smith, N.F., Covey, J.M., Wang, J., and Chan, K.K. (2013). LC-MS/MS quantification of a neuropeptide fragment kisspeptin-10 (NSC 741805) and characterization of its decomposition product and pharmacokinetics in rats. J Chromatogr B Analyt Technol Biomed Life Sci *926*, 1-8.

Livak, K.J., and Schmittgen, T.D. (2001). Analysis of relative gene expression data using real-time quantitative PCR and the 2(-Delta Delta C(T)) Method. Methods *25*, 402-408.

Mortensen, R. (2006). Overview of gene targeting by homologous recombination. Curr Protoc Mol Biol *Chapter 23*, Unit 23 21.

Na, G., Wolfe, A., Ko, C., Youn, H., Lee, Y.M., Byun, S.J., Jeon, I., and Koo, Y. (2013). A low-copy-number plasmid for retrieval of toxic genes from BACs and generation of conditional targeting constructs. Mol Biotechnol *54*, 504-514.

Novaira, H.J., Hoffman, G.E., Koo, Y., Wolfe, A.M., and Radovick, S. (2013). Reproductive abnormalities associated with deletion of Gpr54 in mouse GnRH neurons. Endocrinology suppl.

Petersen, T.N., Brunak, S., von Heijne, G., and Nielsen, H. (2011). SignalP 4.0: discriminating signal peptides from transmembrane regions. Nat Methods *8*, 785-786.

Qureshi, S.A., Rios Candelore, M., Xie, D., Yang, X., Tota, L.M., Ding, V.D., Li, Z., Bansal, A., Miller, C., Cohen, S.M.*, et al.* (2004). A novel glucagon receptor antagonist inhibits glucagon-mediated biological effects. Diabetes *53*, 3267-3273.

Rodriguez, C.I., Buchholz, F., Galloway, J., Sequerra, R., Kasper, J., Ayala, R., Stewart, A.F., and Dymecki, S.M. (2000). High-efficiency deleter mice show that FLPe is an alternative to Cre-loxP. Nat Genet *25*, 139-140.

Smyth, G.K. (2004). Linear models and empirical bayes methods for assessing differential expression in microarray experiments. Stat Appl Genet Mol Biol *3*, Article3.

Song, W.J., Mondal, P., Li, Y., Lee, S.E., and Hussain, M.A. (2013). Pancreatic beta-cell response to increased metabolic demand and to pharmacologic secretagogues requires EPAC2A. Diabetes.

Song, W.J., Seshadri, M., Ashraf, U., Mdluli, T., Mondal, P., Keil, M., Azevedo, M., Kirschner, L.S., Stratakis, C.A., and Hussain, M.A. (2011). Snapin mediates incretin action and augments glucose-dependent insulin secretion. Cell Metab *13*, 308-319.

Subramanian, A., Tamayo, P., Mootha, V.K., Mukherjee, S., Ebert, B.L., Gillette, M.A., Paulovich, A., Pomeroy, S.L., Golub, T.R., Lander, E.S.*, et al.* (2005). Gene set enrichment analysis: a knowledge-based approach for interpreting genome-wide expression profiles. Proc Natl Acad Sci U S A *102*, 15545-15550.